

# A monolithic diode laser chemical sensor with a quasi-symmetrical sensing waveguide for improved sensitivity

C. S. Wang,<sup>a)</sup> J. A. Nolde, D. D. Lofgreen, L. A. Coldren, and D. A. Cohen

*Department of Electrical and Computer Engineering, University of California, Santa Barbara, Santa Barbara, California 93106*

(Received 5 February 2004; accepted 18 May 2004)

We demonstrate a diode laser chemical sensor incorporating a self-aligned, symmetrically clad high index contrast evanescent field sensing waveguide. This is accomplished by selectively oxidizing the lower cladding layer of the sensing waveguide. An analyte overlap of 4.8% is obtained with a tightly confined mode, ideal for sensitive affinity assays. © 2004 American Institute of Physics. [DOI: 10.1063/1.1769080]

There is a growing need for biochemical sensors that are sensitive, fast, small, low powered, and inexpensive for use in medical, industrial, and military applications. To date, some of the highest sensitivities have been demonstrated using interferometric or refractometric techniques, but with nonmonolithic approaches.<sup>1–3</sup> A few monolithically integrated evanescent field sensors have been demonstrated based on waveguide interferometers or on-chip heterodyne detection.<sup>4,5</sup> For optimal sensing of thin chemical layers surface bound to the sensing waveguide, as used in affinity assays, for example, it has been shown that the sensing waveguide must be symmetrically clad, with a large index contrast  $\Delta n$  between core and cladding.<sup>6</sup> Symmetrically clad dielectric waveguides have been demonstrated with a very high sensitivity for bulk sensing, but due to the small index contrast, they offer only modest optical overlap with thin, surface-bound layers.<sup>4</sup> The need for careful alignment between the integrated laser's semiconductor waveguide and the dielectric waveguide also makes fabrication difficult. An all-semiconductor waveguide has also been demonstrated, but the highly asymmetric cladding limited the mode overlap with an analyte to  $\sim 0.02\%$ .<sup>7</sup> In this letter, we report results from, and a process for, fabricating a self-aligned, semiconductor core, quasi-symmetric sensing waveguide that is monolithically integrated with a conventional ridge laser. A 4.8% overlap with an analyte in a tightly confined optical mode is demonstrated.

The major obstacle in constructing a symmetric waveguide is incorporating a low index material below the semiconductor core. In this work, this is accomplished without using a difficult regrowth or etching process, but rather by oxidizing an  $\text{Al}_{0.98}\text{Ga}_{0.02}\text{As}$  layer below the sensing waveguide core. This process is fully self-aligned, resulting in no excess loss from lateral misalignment. The vertical misalignment, to be explained later, resulting from abrupt changes in the refractive index, leads to an increased reflection. However, we use this reflection to build a simple three-mirror resonator,<sup>8</sup> as shown in Fig. 1. The cleave at the front (gain) end, the etched facet at the interface between the gain and sensing regions, and the etched facet at the interface between the sensing and absorber regions comprise the three mirrors. In operation, the absorber region is grounded so that no light

returns from the rear cleaved facet. The net reflectivity is modulated by the resonance in the passive cavity, producing a mode filter whose center wavelength depends on the modal index of refraction in the passive section. This, in turn, is influenced by the evanescent interaction with the medium surrounding the passive waveguide.

The laser itself employs an offset quantum well structure, as shown in the refractive index profile of the layer structure in Fig. 2. The epilayers, grown by molecular beam epitaxy on an  $n$ -GaAs(100) substrate, consist of  $1.4 \mu\text{m} \text{Al}_{0.8}\text{Ga}_{0.2}\text{As}$   $n$ -cladding doped  $1 \times 18 \text{ cm}^{-3}$ ,  $300 \text{ nm} \text{Al}_{0.98}\text{Ga}_{0.02}\text{As}$  oxidation layer doped  $5 \times 17 \text{ cm}^{-3}$   $n$ -type,  $200 \text{ nm} \text{Al}_{0.2}\text{Ga}_{0.8}\text{As}$  waveguide core, graded from  $5 \times 17 \text{ cm}^{-3}$  to unintentionally doped, an active region consisting of three  $8 \text{ nm}$  InGaAs wells with  $8 \text{ nm}$  barriers,  $70 \text{ nm} \text{Al}_{0.3}\text{Ga}_{0.7}\text{As}$   $p$ -SCH ( $5 \times 17 \text{ cm}^{-3}$ ) graded to  $1.4 \mu\text{m} \text{Al}_{0.8}\text{Ga}_{0.2}\text{As}$   $p$ -cladding ( $2 \times 18 \text{ cm}^{-3}$ ), and a  $120 \text{ nm}$  heavily doped  $p$ -GaAs contact layer.

This structure, as grown, has an asymmetrical 1D mode profile, as shown in Fig. 2. With the  $p$ -cladding and active region removed and the  $\text{Al}_{0.98}\text{Ga}_{0.02}\text{As}$  oxidized, a more symmetrical mode results. The  $\text{Al}_x\text{O}_y$  ( $n \approx 1.6$ ) and sensing fluid ( $n \approx 1.3$ ) are thus the low-index cladding layers sandwiching the semiconductor waveguide core. The mode overlap between the active and passive sections is 70%, and the modal power reflectivity is calculated to be 5.8%.

The initial fabrication step was to dry etch down to the waveguide in the middle section, thereby eliminating the absorbing quantum wells and forming a trench for the sensing region. Next, the ridge was patterned perpendicular to the trench and a second dry etch was used to define the ridge structure, which abruptly changes width from  $6 \mu\text{m}$  in the gain and absorber sections to  $2.5 \mu\text{m}$  in the sensing region.

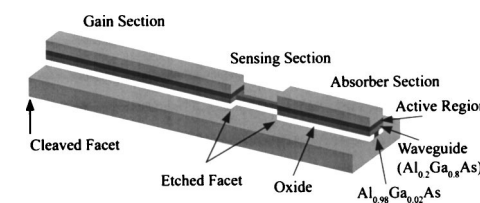


FIG. 1. The device schematic of the coupled-cavity laser sensor. Note the narrower ridge width in the sensing region, allowing complete oxidation beneath the waveguide layer to form a quasi-symmetrically clad waveguide.

<sup>a)</sup>Author to whom correspondence should be addressed; electronic mail: cswang@engineering.ucsb.edu

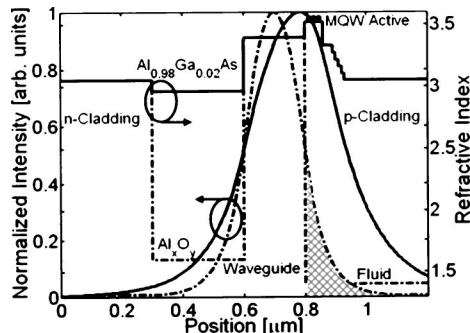


FIG. 2. The labeled epitaxial layer structure of the laser sensor, showing the index of refraction of each layer. The solid line represents the gain section of the laser. The dashed line represents the sensing region, in which the active region has been etched away and the  $\text{Al}_{0.98}\text{Ga}_{0.02}\text{As}$  has been oxidized. Superimposed are the one-dimensional mode profiles of each section. The crosshatched area represents the modal overlap of the evanescent field with the fluid analyte.

The etch penetrated through the waveguide and the 300-nm-thick  $\text{Al}_{0.98}\text{Ga}_{0.02}\text{As}$  layer beneath the waveguide core. A low temperature ( $420^\circ\text{C}$ ) wet oxidation was then used to convert this  $\text{Al}_{0.98}\text{Ga}_{0.02}\text{As}$  layer to  $\text{Al}_x\text{O}_y$ . The oxidation was timed to completely convert the material below the narrow sensing region, but leave an unoxidized width of approximately  $3\ \mu\text{m}$  below the active and absorber waveguides. Similar processes have also been used to fabricate structures utilizing oxide apertures for index and current confinement.<sup>9</sup> Figure 3 shows an SEM image of the gain section with this partial oxidation. This self-aligned process left a high-index-contrast quasi-symmetrically clad waveguide coupled to a more conventional laser waveguide. The gain, sense, and absorber sections were  $400$ ,  $40$ , and  $200\ \mu\text{m}$  long, respectively. The process was completed with Ti/Pt/Au *p*-contacts and AuGe/Ni/Au *n*-contacts on the back of the thinned substrate. The devices were cleaved and mounted onto copper studs for pulsed testing. Pulse testing was used to avoid self-heating in the device, which would skew the data.

To measure the mode overlap with an analyte, the entire device was submerged in a temperature-controlled bath of fluid held at  $18 \pm 0.1^\circ\text{C}$ , monitored with a thermistor. The bath was covered to minimize evaporative cooling. The gain

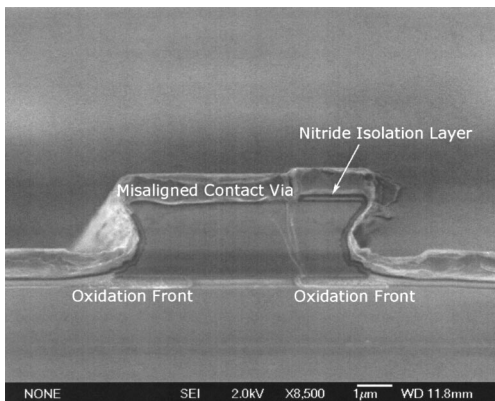


FIG. 3. The scanning electron micrograph of a cross section of the gain region. The oxidation front can be seen approaching from both sides of the etched sidewall, leaving a  $3\ \mu\text{m}$  wide current path through the  $\text{Al}_{0.98}\text{Ga}_{0.02}\text{As}$ . The defect running from the oxidation front to the misaligned nitride layer on top of the ridge is possibly due to strain between these two layers.

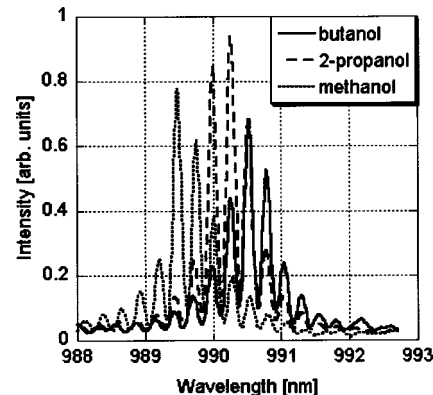


FIG. 4. The lasing spectra for three different fluids bathing the sensor. The mode filter center wavelength depends on the fluid index of refraction, and is found by interpolation between the dominant modes.

section was biased at  $45\ \text{mA}$ ,  $5\ \text{mA}$  above the threshold, with  $500\ \text{ns}$  pulses at a repetition rate of  $10\ \text{kHz}$ . Five different alcohol mixtures were tested; for clarity, only three of the lasing spectra are shown in Fig. 4. An interpolation scheme was used to determine the filter center wavelength from the intensities of the three strongest lasing modes:

$$\lambda_c = \lambda_o + \left( \frac{P_{+1} - P_{-1}}{P_{+1} + P_{-1}} \right) \left( \frac{\lambda_{+1} - \lambda_o}{2} \right), \quad (1)$$

where  $\lambda_c$  is the center wavelength,  $\lambda_o$  is the dominant mode wavelength,  $\lambda_{\pm 1}$  are the wavelengths of modes adjacent to  $\lambda_o$ , and  $P_{\pm 1}$  are the powers of modes adjacent to  $\lambda_o$ . As shown in Fig. 5, this filter wavelength shifted nearly linearly with the index of refraction of the bathing fluid. The modal overlap with the fluid to be sensed,  $\Gamma$ , is related to the filter wavelength by,

$$\frac{\Delta\lambda_c}{\lambda_c} = \Gamma \frac{\Delta n_{\text{fluid}}}{n_{\text{eff}}}, \quad (2)$$

where  $\Delta\lambda_c$  is the shift in  $\lambda_c$  due to a shift in fluid index  $\Delta n_{\text{fluid}}$ , and  $n_{\text{eff}}$  is the modal effective index in the passive section. From the data,  $\Gamma$  was calculated to be  $4.8\%$ , a hundredfold improvement over previous work with an asymmetrically clad waveguide and in good agreement with two-dimensional mode simulations of  $4.45\%$ .

In conclusion, we have developed a manufacturable technique to monolithically couple symmetrically clad high index contrast waveguides to conventional semiconductor la-

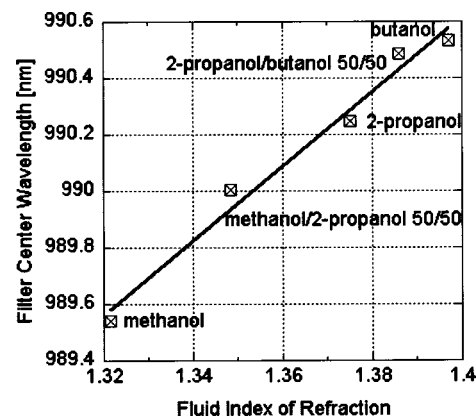


FIG. 5. The filter center wavelength as a function of the fluid index of refraction. All fluid indices were measured with an Abbe refractometer.

ser waveguides. The tight optical confinement is ideal for the sensing of thin analyte layers surface bound to the sensing waveguide. Integration of this structure into sensors based on either interferometric or heterodyne detection would yield femtogram sensitivities from picoliter volumes.

This work was supported by DARPA within the Bioflips and Simbiosys programs under Contract Nos. DAAD 19-00-1-0400 and F30602-01-2-0538.

<sup>1</sup>R. G. Heidemann and P. V. Lambeck, *Sens. Actuators B* **B61**, 100 (1999).

<sup>2</sup>C. F. R. Mateus, M. C. Y. Huang, J. E. Foley, R. Beatty, C. J. Chang-

Hasnain, P. Li, and B. Cunningham, LEOS 16th Annual Meeting, paper no. PD 2.4, Tucson, AZ (2003).

<sup>3</sup>W. Lukosz, *Sens. Actuators B* **B29**, 37 (1995).

<sup>4</sup>B. Maisenhölder, H. P. Zappe, R. E. Kunz, P. Riel, M. Moser, and J. Edlinger, *Sens. Actuators B* **38–39**, 324 (1997).

<sup>5</sup>D. A. Cohen, E. J. Skogen, H. Marchand, and L. A. Coldren, *Electron. Lett.* **37**, 1358 (2001).

<sup>6</sup>O. Parriaux and G. J. Veldhuis, *J. Lightwave Technol.* **16**, 573 (1998).

<sup>7</sup>D. A. Cohen, J. A. Nolde, A. Tauke Pedretti, C. S. Wang, E. J. Skogen, and L. A. Coldren, *IEEE J. Sel. Top. Quantum Electron.* **9**, 1124 (2003).

<sup>8</sup>L. A. Coldren and S. W. Corzine, *Diode Lasers and Photonic Integrated Circuits* (Wiley, New York, 1995), p. 79.

<sup>9</sup>S. A. Maranowski, A. R. Sugg, E. I. Chen, and N. Holonyak, Jr., *Appl. Phys. Lett.* **63**, 1660 (1993).